

DISCOVERY OF GLOBULAR CLUSTERS IN THE PROTO-SPIRAL NGC 2915: IMPLICATIONS FOR HIERARCHICAL GALAXY EVOLUTION

GERHARDT R. MEURER¹, J.P. BLAKESLEE¹, M. SIRIANNI¹, H.C. FORD¹, G.D. ILLINGWORTH², N. BENÍTEZ¹, M. CLAMPIN³, F. MENANTEAU¹, H.D. TRAN⁴, R.A. KIMBLE³, G.F. HARTIG⁵, D.R. ARDILA¹, F. BARTKO⁶, R.J. BOUWENS¹, T.J. BROADHURST⁷, R.A. BROWN⁵, C.J. BURROWS⁵, E.S. CHENG³, N.J.G. CROSS¹, P.D. FELDMAN¹, D.A. GOLIMOWSKI¹, C. GRONWALL⁸, L. INFANTE⁹, J.E. KRIST⁵, M.P. LESSER¹⁰, A.R. MARTEL¹, G.K. MILEY¹¹, M. POSTMAN⁵, P. ROSATI¹², W.B. SPARKS⁵, Z.I. TSVETANOV¹, R.L. WHITE^{1,5}, & W. ZHENG¹
ApJ Letters, accepted

ABSTRACT

We have discovered three globular clusters beyond the Holmberg radius in Hubble Space Telescope Advanced Camera for Surveys images of the gas-rich dark matter dominated blue compact dwarf galaxy NGC 2915. The clusters, all of which start to resolve into stars, have $M_{V606} = -8.9$ to -9.8 mag, significantly brighter than the peak of the luminosity function of Milky Way globular clusters. Their colors suggest a metallicity $[Fe/H] \approx -1.9$ dex, typical of metal-poor Galactic globular clusters. The specific frequency of clusters is at a minimum normal, compared to spiral galaxies. However, since only a small portion of the system has been surveyed it is more likely that the luminosity and mass normalized cluster content is higher, like that seen in elliptical galaxies and galaxy clusters. This suggests that NGC 2915 resembles a key phase in the early hierarchical assembly of galaxies - the epoch when much of the old stellar population has formed, but little of the stellar disk. Depending on the subsequent interaction history, such systems could go on to build-up larger elliptical galaxies, evolve into normal spirals, or in rare circumstances remain suspended in their development to become systems like NGC 2915.

Subject headings: galaxies: star clusters — galaxies: individual (NGC 2915) — galaxies: evolution — galaxies: halos

1. INTRODUCTION

All galaxies with massive old stellar populations are thought to contain globular clusters (GCs). They are particularly noticeable where the old stellar population is dominant such as in elliptical (E), dwarf elliptical (dE), and central Dominant (cD), as well as spiral galaxies with prominent bulges. Dwarf spheroidal galaxies generally do not contain GCs, probably because they have insufficient mass to make their formation likely. The exceptions are the most massive dwarf spheroidals Fornax (Hodge 1961) and Sagittarius (Ibata, Gilmore & Irwin 1994) which each have at least 4 GCs. Disk galaxies dominated by population I stars contain fewer GCs per unit luminosity, presumably because of star formation in the disk after the formation of the population II component. Galaxies with a high M_{HI}/L_B ratio have yet to form much of their baryonic mass into stars. They typically are blue and not considered likely hosts for populous GC systems.

NGC 2915 is an extreme gas rich galaxy having $M_{HI}/L_B = 1.7 M_{\odot}/L_{B,\odot}$ (Meurer *et al.* 1996, hereafter MCBF96). Its regularly rotating HI disk extends to over 5 times beyond the readily detectable optical emission providing an excellent

dynamical tracer for the mass distribution; not coincidentally NGC 2915 has one of the highest known mass-to-light ratios in a single galaxy (MCBF96). Furthermore, while its optical morphology is that of a blue compact dwarf (BCD; Meurer, Mackie, & Carignan 1994, hereafter MMC94), its HI disk clearly shows spiral arms which are not apparent in the optical.

In this Letter, we report the discovery of three luminous GCs found in Hubble Space Telescope Advanced Camera for Surveys (ACS; Ford *et al.* 2002) images of NGC 2915 that were obtained in order to look for a stellar heating source for the HI disk. That issue will be discussed in a separate article (Meurer *et al.* 2003; in preparation, hereafter Meu03).

2. DATA AND ANALYSIS

ACS Wide Field Camera (WFC) images were obtained of a field centered at $09^h 25^m 36^s.48$, $-76^{\circ} 35' 52''.4$ (J2000). The images cover projected radii of $45''$ to $257''$, whereas the Holmberg radius $R_{Ho} = 114''$. We obtained 2, 2, 4 images for a total exposure of 2480s, 2600s, 5220s in the filters F475W (g_{475}), F606W (V_{606}), and F814W (I_{814}), respectively. The basic processing of the images was done using the CALACS pipeline (Hack 1999). We used the program *Apsis* (Blakeslee *et al.*

¹ Department of Physics and Astronomy, The Johns Hopkins University, 3400 North Charles Street, Baltimore, MD 21218; meurer@pha.jhu.edu

² UCO/Lick Observatory, University of California, Santa Cruz, CA 95064.

³ NASA Goddard Space Flight Center, Greenbelt, MD 20771.

⁴ W.M. Keck Observatory, 65-1120 Mamalahoa Hwy., Kamuela, HI 96743

⁵ STScI, 3700 San Martin Drive, Baltimore, MD 21218.

⁶ Bartko Science & Technology, P.O. Box 670, Mead, CO 80542-0670.

⁷ Racah Institute of Physics, The Hebrew University, Jerusalem, Israel 91904.

⁸ Department of Astronomy and Astrophysics, The Pennsylvania State University, 525 Davey Lab, University Park, PA 16802.

⁹ Departamento de Astronomía y Astrofísica, Pontificia Universidad Católica de Chile, Casilla 306, Santiago 22, Chile.

¹⁰ Steward Observatory, University of Arizona, Tucson, AZ 85721.

¹¹ Leiden Observatory, Postbus 9513, 2300 RA Leiden, Netherlands.

¹² European Southern Observatory, Karl-Schwarzschild-Strasse 2, D-85748 Garching, Germany.

2002) to align and combine the images incorporating geometric correction and rejection of cosmic rays and hot pixels.

Here we present photometry in the natural system of the filters, with zeropoints selected so that Vega would have a magnitude of 0.0 in all bands. In order to compare our observations with previous work, we convert the previous work to this system, as needed, using the calibrations of Sirianni et al (2003, in preparation). The most important correction is to the V_{606} photometry, since the F606W filter straddles the wavelength of traditional V and R filters.

3. RESULTS

Table 1 presents adopted global properties for NGC 2915. The foreground extinction, $E(B-V)$, is from the Schlegel, Finkbeiner & Davis (1998) extinction maps. It is significantly larger than $E(B-V) = 0.15 \pm 0.05$ estimated by MMC94, but consistent with the position of the field star Red Giant Branch (RGB; Meu03). Extinction corrected photometry employing the Cardelli, Clayton & Mathis (1989) extinction curve is denoted with a “0” subscript. The distance, D was derived from the field star RGB tip (Meu03). It is consistent with but improves on previous estimates $D = 5.3 \pm 1.3$ Mpc (MMC94) and $D = 3.8 \pm 0.5$ Mpc (Karachentsev *et al.* 2003). The remaining quantities in Table 1 were derived from MMC94 and MCBF96 after correcting to the new $E(B-V)$ and D .

As shown in Fig. 1, the three sources are clearly GCs whose brightest stars are resolved. Table 2 compiles the properties of the clusters. The photometric quantities were measured using a circular aperture having a radius of $r = 3''$, with the local sky subtracted using an annulus having radii of $5''$ and $7.5''$. The cluster size $r_{1/2}$ is the circular aperture radius encompassing half the V_{606} light as measured from curves of growth.

Compared to Galactic GCs, these clusters are large and luminous, but not abnormally so. Only 16% of the clusters in the Harris (1996) database¹³ have V_{606} luminosities brighter than G3; only three clusters are more luminous than G1. The clusters’ $r_{1/2}$ ranges from about 5 to 9 pc, placing them in the upper quartile of Galactic GCs which have $r_{1/2}$ ranging from 0.3 to 24.7 pc (Harris 1996). The clusters are noticeably elongated with ellipticity $\epsilon \equiv 1 - b/a$ similar to the canonical flattened Galactic GCs M22 and ω Cen ($\epsilon = 0.14, 0.17$, respectively; Harris 1996). The combination of high luminosity and appreciable flattening is also seen in the cluster M31-G1 (Pritchet & van den Bergh 1984; Meylan *et al.* 2001).

The $(g_{475} - V_{606})_0$ and $(V_{606} - I_{814})_0$ colors of the clusters are compared to Milky Way GCs (Harris 1996) in Fig. 2. Their colors are virtually identical implying similar metallicities, assuming they are old and nearly coeval. We derive their metallicity by fitting the metallicity - color relationship from the Harris database after converting the colors to $(V_{606} - I_{814})_0$. We employed an unweighted least squares fit with an iterative 2.5σ rejection resulting in $[\text{Fe}/\text{H}] = -5.37 + 5.36(V_{606} - I_{814})_0$ with a dispersion of 0.29 dex. The metallicity for the three clusters is then $[\text{Fe}/\text{H}] = -1.9 \pm 0.4$ dex, consistent with *low* metallicity Galactic GCs. Our stellar population analysis, in progress (Meu03), indicates that the stars at the outskirts of the clusters have very similar $I_{814,0}$ versus $(V_{606} - I_{814})_0$ color-magnitude diagrams, dominated by a narrow and blue RGB. This is also consistent with low $[\text{Fe}/\text{H}]$, if the clusters are old.

4. DISCUSSION

4.1. Cluster formation efficiency

Because of the blue core and gas rich nature of NGC 2915 we had not expected to find GCs in our images. However, in retrospect this discovery should not have been surprising. GCs have previously been discovered around morphologically similar systems; Östlin, Bergvall & Rönnback (1998) find a considerable population of at least 65 old GCs about the Blue Compact (albeit not dwarf) galaxy ESO 338-IG04. In addition, NGC 2915 is not a dwarf system in terms of mass, and optical imaging shows that it to be dominated by an older stellar population for $R > 0.5$ Kpc (MMC94). These facts suggest that old GCs might have been expected.

Are the number of clusters found anomalous? To address this we estimate the total number of clusters in the system. Unfortunately, our images sample only a small fraction of the galaxy. If the GCs are distributed spherically out to $R_{\text{HI}} = 10'$ (where the H I distribution ends; MCBF96), then we have only surveyed 3.5% of the available area. Here we consider two cases for the possible distribution of old clusters. Case (1) assumes that we are lucky and have managed to observe all the clusters in NGC 2915. While this is unlikely, it provides a strict lower limit to the cluster formation efficiency. The more likely case (2) is that the globular cluster system is like that of more luminous systems - having a spherically symmetric power-law radial distribution in number per unit area - $N(R) \propto R^\alpha$ (Harris 1991). We assume this extends between $R = 0.5$ Kpc and R_{HI} , where the minimum R insures that the predictions are finite and was chosen to correspond to the size of the central star forming population (MMC94). For $-2.5 < \alpha < -0.5$ we estimate that the total number of clusters in the system is 7 to 12 times higher than found on our images. For case (2) we adopt a correction factor of 9. Hence there are at least 3 GCs in the system (case 1), with a more likely number being ~ 27 (case 2).

In principle, we should correct the total GC estimate for the finite luminosity sampling of the images. However, SExtractor (Bertin & Arnouts 1996) catalogs of our images show that we can detect extended objects down to $V_{606} \approx 27$ which corresponds to an $M_{V_{606}} \sim -2$ for sources in NGC2915. This is well below the peak of the GC luminosity function $M_V \sim -7.5$ (Secker 1992; revised to agree with the *Hipparcos* RR Lyrae zero point, e.g. Carretta *et al.* 2000). Hence we apply no luminosity sampling correction. The fact that we only have found GCs much brighter than this peak is somewhat puzzling.

We will consider three measures of cluster formation efficiency. First, the specific frequency, $S_N = N_T 10^{0.4(M_V+15)}$, is the V luminosity normalized cluster content (Harris & van den Bergh 1981). S_N is typically around 1 for spiral galaxies and increases towards earlier galaxy types, with E galaxies having $S_N \sim 4$. In the center of galaxy clusters S_N ranges from 2.5 to 12.5 (Blakeslee, Tonry, & Metzger 1997; Blakeslee 1999). We consider two measures of the mass normalized contribution: η_{GC} the number of clusters per $10^9 M_\odot$ in dynamical mass (Blakeslee *et al.* 1997), and ϵ_{cl} , the fractional baryonic (gas and stars) mass in GCs (McLaughlin 1999). As done by McLaughlin (1999) we assume each cluster has an average mass $\langle M_{\text{cl}} \rangle = 2.4 \times 10^5 M_\odot$ when calculating ϵ_{cl} . Blakeslee *et al.* (1997) find an average $\eta_{\text{GC}} = 0.7$ with a scatter of 30%, while McLaughlin (1999) computes an average $\epsilon_{\text{cl}} = 0.0026$ with a 20% uncertainty.

Table 3 tabulates S_N , η_{GC} and ϵ_{cl} for NGC 2915 under the above two cases. Relevant quantities used for these calculations

¹³ <http://physwww.physics.mcmaster.ca/~harris/mwgc.dat>

are given in Table 1. Table 3 also lists literature values and uncertainties of the efficiencies for “normal” systems. The uncertainty of our estimates are large: for a Poissonian distribution yielding a count of 3, the 95% confidence limits on the cluster formation efficiencies are 0.3 and 2.3 times the estimated value. We find that at a minimum (case 1) S_N is close to normal for a spiral galaxy while η_{GC} and ϵ_{cl} are low compared to normal globular cluster systems. In the more likely case (2), S_N is very high compared to normal gas rich systems. η_{GC} and ϵ_{cl} are also somewhat high compared to literature values, but in reasonable agreement considering the Poissonian uncertainty of our measurements. While we can not rule out the possibility that NGC 2915 is like a normal spiral galaxy in terms of S_N , it is more likely that it has a high luminosity normalized cluster content, whereas the mass normalized content is closer to normal.

4.2. A missing link in galaxy evolution?

It is interesting to interpret these results within the framework of hierarchical evolution through comparison with other systems. Blakeslee (1999) has discussed how the S_N of the young Milky Way must have been fairly high, similar to the values for cluster E galaxies, after the formation of the Galactic halo but before stellar disk formation. The increase in luminosity from later star formation in the disk would cause a decrease in the Galactic S_N to its present low value, while leaving the number of GCs per unit mass unchanged. In NGC 2915 we have an example of a present-day galaxy with an old stellar component, including GCs, but a spiral disk that is still mainly in the form of gas.

In this sense, NGC 2915, like the centers of rich galaxy clusters, has an elevated value of S_N compared to typical spirals because of a lower efficiency for converting gas into stars. Clusters typically have 2–5 times as much mass in gas as in stars (Arnaud *et al.* 1992), similar to what we see in NGC 2915. The difference, however, is that the gas in clusters now resides in the hot intracluster medium, while the gas in NGC 2915 still retains the potential to be converted into stars. To a large extent, the fate of the gaseous disk (and the future evolution of S_N in NGC 2915) must depend on the surrounding environment.

Simulations show that when a disk galaxy enters the environment of a rich galaxy cluster, much of the gas in its disk and halo will be removed by the combination of tidal and ram pressure stripping (Abadi, Moore & Bower 1999; Bekki, Couch & Shioya 2002; Bekki *et al.* 2001; Gnedin 2003). For example, if a system similar to the Galaxy were to fall into a rich cluster it would have its gas disk truncated down to a radius of a few kpc within a few tens of Myr by ram pressure stripping alone (Abadi

et al. 1999). Indeed, models of present day evolution of galaxy clusters invoke mildly truncated star formation in field galaxies accreting onto the cluster as the cause of the Butcher-Oemler effect (Balogh, Navarro & Morris 2000; Kodama & Bower 2001). It is likely that in their *early evolution* clusters were assembled from building blocks similar to NGC 2915 which had their ISM stripped from them by these mechanisms. The stripped gas was then virialized to become the cluster X-ray halo. In this scenario galaxy clusters have high S_N because they formed out of subclumps which had already efficiently formed star clusters but which never had the chance to form disks.

In a less hostile environment, a building block similar to NGC 2915 could go on to form a normal spiral galaxy. If the H I disk of NGC 2915 were to be perturbed enough to efficiently form stars in a fairly quiescent fashion this would result in an additional $7 \times 10^8 M_\odot$ of stars forming with no additional GCs. Assuming a $M/L_V \sim 1 M_\odot/L_{V,\odot}$ for the additional stars then the system would evolve towards $S_N \sim 2$, a fairly normal value for spiral galaxies, while η_{GC} and ϵ_{cl} remain fixed at their normal values. The S_N in NGC 2915 is then anomalously high because the formation of its disk has not proceeded, presumably due to a lack of external perturbations (MCBF96). If so, then we may expect other galaxies with high M_{HI}/L_B ratios and extended H I disks to also have a significant GC population, especially if they have a strong old population.

While this scenario seems compelling, we caution that it is possible that NGC 2915 only superficially resembles the building block we describe. We have not proven that the number of clusters is anomalously high. Furthermore, we can not yet rule out the possibility that the clusters are of higher metallicity and younger than Galactic GCs. This is shown in figure 2 where we overplot Bruzual & Charlot (2003) population models on the two color diagram illustrating the strong age-metallicity degeneracy for the filters used here. If the clusters are not old, they may represent the remnants of a starburst occurring as recently as a few Gyr ago. We are undertaking additional observations (imaging and spectroscopic) to get a more accurate census of star clusters in the NGC 2915 system and determine their nature. The results of these studies should determine whether NGC 2915 is just a gas rich galaxy with a peculiar star formation history, or whether it truly presents us with a rare local view of how galaxies looked in the epoch of cluster assembly.

ACS was developed under NASA contract NAS 5-32864, and this research has been supported by NASA grant NAG5-7697. We thank the technical and administrative support staff of the ACS science team for their committed work on the ACS project.

REFERENCES

- Abadi, M.G., Moore, B., & Bower, R.G. 1999, MNRAS, 308, 947
 Arnaud, M., Rothenflug, R., Boulade, O., Vigroux, L., & Vangioni-Flam, E. 1992, A&A, 254, 49
 Balogh, M.L., Navarro, J.F. & Moore, S.L. 2000, ApJ, 540, 113
 Bekki, K., Couch, W.J., Drinkwater, M.J., & Gregg, M.D. 2001, ApJ, 557, L39
 Bekki, K., Couch, W.J., & Shioya, Y. 2002, ApJ, 577, 651
 Bertin, E. & Arnouts, S. 1996, A&AS, 117, 393
 Blakeslee, J.P. 1999, AJ, 118, 1506
 Blakeslee, J.P., Tonry, J.L., & Metzger, M.R. 1997, AJ, 114, 482
 Blakeslee, J.P., Anderson, K.R., Meurer, G.R., Benitez, N., & Magee, D. 2002, ASP Conf. Ser. 295: ADASS XII, 257
 Bruzual, G., & Charlot, S. 2003, MNRAS, in press (astro-ph/0309134)
 Cardelli, J.A., Clayton, G.C., & Mathis, J.S. 1989, ApJ, 345, 245
 Carretta, E., Gratton, R.G., Clementini, G., & Fusi Pecci, F. 2000, ApJ, 533, 215
 Ford, H.C., *et al.* 2002, Proc. SPIE, 4854, 81
 Gnedin, O.Y. 2003, ApJ, 589, 752
 Hack, W.J. 1999, CALACS Operation and Implementation, ISR ACS-99-03 (Baltimore: STScI)
 Harris, W.E. & van den Bergh, 1981, AJ, 86, 1627
 Harris, W.E. 1991, ARA&A, 29, 543
 Harris, W.E. 1996, AJ, 112, 1487
 Hodge, P.W. 1961, AJ, 66, 83
 Ibata, R., Gilmore, G., & Irwin, M. 1994, Nature, 370, 194
 Kodama, T. & Bower, R.G. 2001, MNRAS, 321, 18
 Karachentsev, *et al.* 2003, A&A, 398, 479
 McLaughlin, D.E. 1999, AJ, 117, 2398
 Meurer, G.R., Mackie, G., & Carignan, C. 1994, AJ, 107, 2021 (MMC94)
 Meurer, G.R., Carignan, C., Beaulieu, S., & Freeman, K.C. 1996, AJ, 111, 1551 (MCBF96)

Meylan, G., Sarajedini, A., Jablonka, P., Djorgovski, S.G., Bridges, T., & Rich,
R.M. 2001, AJ, 122, 830
Östlin, G., Bergvall, N., & Rönnback, J. 1998, A&A, 335, 85

Pritchett, C.J., & van den Bergh, S. 1984, PASP, 96, 804
Secker, J. 1992, AJ, 104, 1472
Schlegel, D.J., Finkbeiner, D.P., & Davis, M. 1998, ApJ, 500, 525

TABLE 1
 NGC 2915 PROPERTIES

Quantity	Value	Units	Description
$E(B-V)$	0.28 ± 0.04	mag	foreground extinction
D	4.1 ± 0.3	Mpc	Distance
\mathcal{M}_g	7.4×10^8	\mathcal{M}_\odot	ISM mass
\mathcal{M}_*	3.2×10^8	\mathcal{M}_\odot	Mass in stars
\mathcal{M}_T	2.1×10^{10}	\mathcal{M}_\odot	Total dynamical mass
M_V	-16.42	mag	Absolute mag V band
L_B	3.4×10^8	$L_{B,\odot}$	B band luminosity
\mathcal{M}_T/L_B	62	solar	Mass to light ratio

 TABLE 2
 CLUSTER PROPERTIES

ID	RA ^a (J2000)	Dec ^a (J2000)	R (kpc)	M_{V606}	$(g_{475}-V_{606})_0$	$(V_{606}-I_{814})_0$	$r_{1/2}$ (pc)	ϵ
G1	09 25 56.273	-76 35 14.53	3.0	-9.82	0.62	0.66	8.8	0.11
G2	09 25 27.445	-76 36 31.55	3.3	-9.04	0.57	0.65	4.6	0.16
G3	09 25 41.954	-76 36 33.70	2.4	-8.92	0.59	0.64	5.9	0.13

^aThe absolute accuracy of the positions $\sim 0''.2$ in each coordinate is set by the astrometric calibration which employed 86 stars in the HST Guide Star Catalog version 2 (<http://www-gsss.stsci.edu/gsc/gsc2/GSC2home.htm>). The relative accuracy of the positions is $< 0''.05$ in each coordinate.

 TABLE 3
 GLOBULAR CLUSTER SYSTEM PROPERTIES

Quantity	Case (1)	Case (2)	Literature
S_N	0.81	7.3	0–12.5
η_{GC}	0.14	1.3	0.7 ± 0.2
ϵ_{cl}	0.00067	0.0061	0.0026 ± 0.0005



FIG. 1.— Three color images of the three globular clusters; from left to right: G1, G2, G3. The images are shown on the same logarithmic stretch, with F814W, F606W, and F475W representing red, green and blue respectively. Each image is $8''$ on a side and has the same orientation. The large arrow of the compass in the middle panel points to north, the small arrow points to east.

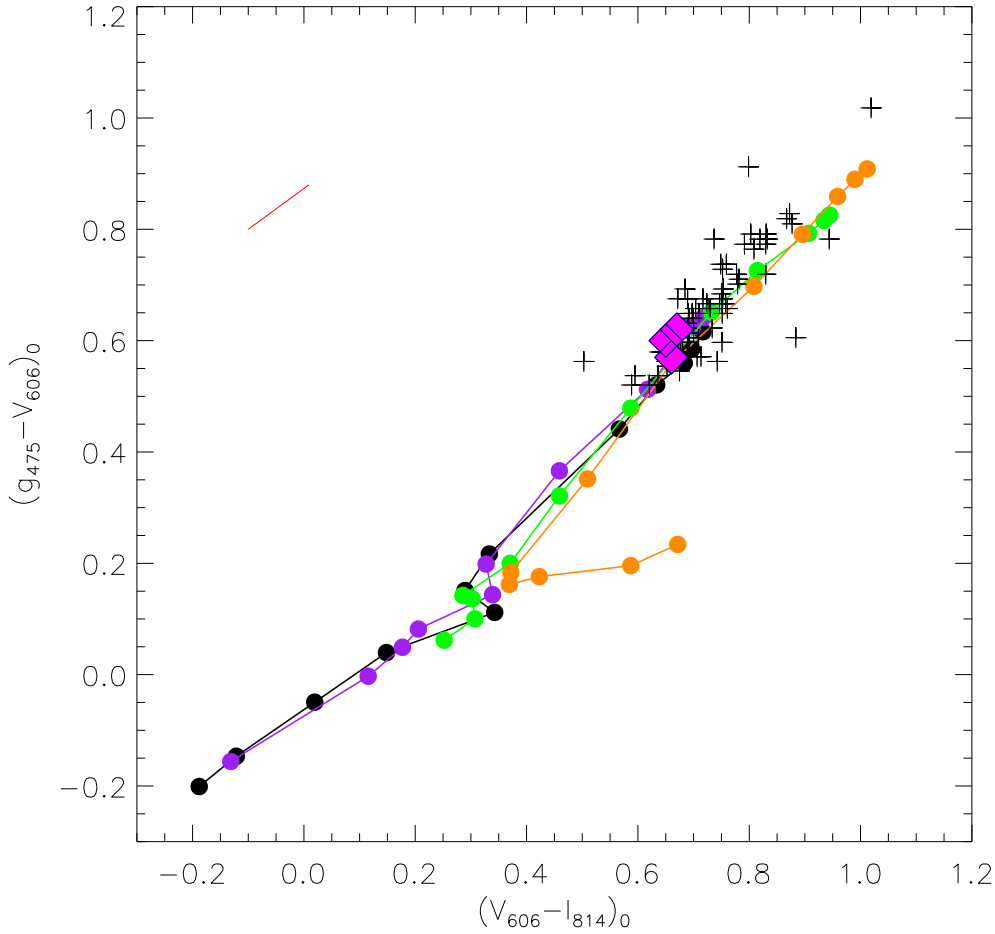


FIG. 2.— Color-color plots of the NGC 2915 globular clusters (pink filled diamonds) compared to Galactic globular clusters (crosses; from Harris 1996), and “simple stellar population” models from Bruzual & Charlot (2003; colored connected dots). All data have been corrected for Galactic extinction. The red line segment shows the $E(B-V) = 0.1$ reddening vector (Cardelli *et al.* 1999). Population models having ages of 0.01, 0.02, 0.05, 0.1, 0.2, 0.5, 1.0, 2.0, 5.0, 10, 15, and 20 Gyr are plotted in four constant metallicity model sequences having $[\text{Fe}/\text{H}] = -2.25$ (black); -1.65 (purple); -0.33 (green); and 0.09 (orange). All models employ the standard stellar evolution and Initial Mass Function prescriptions from Bruzual & Charlot (2003).